

Temperature and doping dependence of high-energy kink in cuprates

M. M. Zemljčič¹, P. Prelovšek^{1,2} and T. Tohyama³

¹*J. Stefan Institute, SI-1000 Ljubljana, Slovenia*

²*Faculty of Mathematics and Physics, University of Ljubljana, SI-1000 Ljubljana, Slovenia and*

³*Yukawa Institute for Theoretical Physics, Kyoto University, Kyoto 606-8502, Japan*

(Dated: October 31, 2018)

It is shown that spectral functions within the extended t - J model, evaluated using the finite-temperature diagonalization of small clusters, exhibit the high-energy kink in single-particle dispersion consistent with recent angle-resolved photoemission results on hole-doped cuprates. The kink and waterfall-like features persist up to large doping and to temperatures beyond J hence the origin can be generally attributed to strong correlations and incoherent hole propagation at large binding energies. In contrast, our analysis predicts that electron-doped cuprates do not exhibit these phenomena in photoemission.

PACS numbers: 71.27.+a, 75.20.-g, 74.72.-h

The anomalous properties of quasiparticles (QP) in cuprates are most directly probed by the angle-resolved photoemission spectroscopy (ARPES) [1]. Besides the Fermi surface development, pseudogap features and low-energy kink [1] considerable attention has been recently devoted to the high-energy kink (HEK) observed by ARPES quite universally in hole-doped cuprates [2, 3, 4, 5, 6, 7, 8, 9, 10]. The anomaly appears in the QP dispersion along the zone diagonal $(0, 0) - (\pi/2, \pi/2)$ as a kink at binding energies typically $E_1 \sim 0.4$ eV followed by a fast drop - 'waterfall' to the high-energy scale $E_2 \sim 1$ eV being well pronounced around the zone center $\mathbf{k} \sim (0, 0)$. The HEK seems to exist in a broad range of hole-doped cuprates: from undoped [2, 3], underdoped [3, 4, 5], optimally doped [3, 4, 5, 6], overdoped [3, 4, 7, 8] to highly overdoped regime [3, 9]. Some ARPES spectra [4, 7] give indications for the coexistence of two branches in the part of the Brillouin zone: one representing the renormalized QP band reaching $E \sim E_1$ and the second being the remnant of the high-energy unrenormalized band at $E \sim E_2$. Analogous evidence for the HEK in electron-doped cuprates [7, 10] is less conclusive.

Theoretically, the origin of the HEK is presently lively debated. Since in contrast to low-energy kink [1] the energy E_1 is too high to be attributed to phonons, several aspects of strong correlations are given as a possible explanation. The similarity to spectral functions of one-dimensional (1D) chain cuprate SrCuO₂ [11] with pronounced two component spectra, i.e., spinon and holon branches, seems to support the long-sought spinon-holon scenario also for two-dimensional (2D) cuprates [4]. On the other hand, alternative explanations with string excitations of a QP in an antiferromagnet (AFM) [12], split QP band within the slave-boson theory [13], and the vicinity to a quantum critical point [14] are not restricted to 1D. Recent numerical calculations within the Hubbard model support the existence of the HEK in prototype models of correlated electrons, both for the undoped system [15] as well as in the large-doping regime [16], where the origin of HEK is attributed to high-energy spin correlations [16, 17].

In the following we present finite-temperature numerical results within the prototype t - J model of strongly correlated

electrons in cuprates. They reveal the existence of the HEK in a broad range of hole concentration c_h and temperature T in the $\omega < 0$ sector of spectral functions $A(\mathbf{k}, \omega)$, corresponding to ARPES in hole-doped cuprates. Well pronounced at intermediate and large doping as the waterfall-like dispersion, the HEK develops at lower doping and $T < J$ into two partly coexisting branches, the renormalized QP band and a broad bottom band. An important fact for the interpretation is the observed persistence of the HEK up to high $T \sim t > J$ which gives strong support to the scenario that the HEK and waterfall are quite universal signatures of strong correlations and only indirectly connected to low- T phenomena as the longer-range AFM and superconductivity in these materials. Also, strong asymmetry in ω leads to the conclusion that analogous phenomena in electron-doped cuprates should be absent within ARPES spectra.

We study the single-particle excitations within the extended t - J model

$$H = - \sum_{i,j,s} t_{ij} \tilde{c}_{js}^\dagger \tilde{c}_{is} + J \sum_{\langle ij \rangle} \mathbf{S}_i \cdot \mathbf{S}_j, \quad (1)$$

where \tilde{c}_{is}^\dagger are projected fermionic operators not allowing for the double occupancy of sites. As relevant for cuprates we consider the model on a square lattice and include besides the nearest-neighbor $t_{ij} = t$ also the second-neighbor $t_{ij} = t'$ and the third-neighbor hopping $t_{ij} = t''$. We present in the following results for $t' = -0.25 t$, $t'' = 0.12 t$, $J = 0.4 t$ [18, 19] chosen to reproduce well properties of hole-doped cuprates, e.g., the measured Fermi surface.

We calculate the spectral function $A(\mathbf{k}, \omega)$ using the usual $T = 0$ exact diagonalization method and the finite-temperature Lanczos method (FTLM) for $T > 0$ [20]. Systems considered here are tilted square lattices of $N = 18, 20$ sites with finite concentration of holes $c_h = N_h/N$ doped into the reference undoped AFM insulator. Since fixed boundary conditions on small systems allow only a discrete set of wavevectors \mathbf{k}_l , $l = 1, N$ we employ twisted boundary conditions to scan the whole Brillouin zone [19], $\mathbf{k} = \mathbf{k}_l + \vec{\theta}$ by introducing hopping elements $t_{ij} \rightarrow \tilde{t}_{ij} = t_{ij} \exp(i\vec{\theta} \cdot \vec{r}_{ij})$ in Eq. (1). For details of the application of the FTLM to spectral

functions we refer to Ref.[21]. Besides the evident possibility of obtaining $T > 0$ results the FTLM allows for a reliable evaluation of the self energy $\Sigma(\mathbf{k}, \omega)$ which is essential for the interpretation of observed phenomena.

First we present results for $A(\mathbf{k}, \omega)$ at hole-doping $c_h = 0.1$ corresponding to underdoped regime calculated on a system of $N = 20$ sites. In Fig. 1 we present the weight map of $A(\mathbf{k}, \omega)$ along the diagonal and the edge directions within the first Brillouin zone and its evolution with increasing T . The $T = 0$ result in Fig. 1a is obtained by the ground state Lanczos procedure [19], while in Fig. 1b,c,d FTLM results are shown for increasing $T/t = 0.2, 0.4, 0.75$.

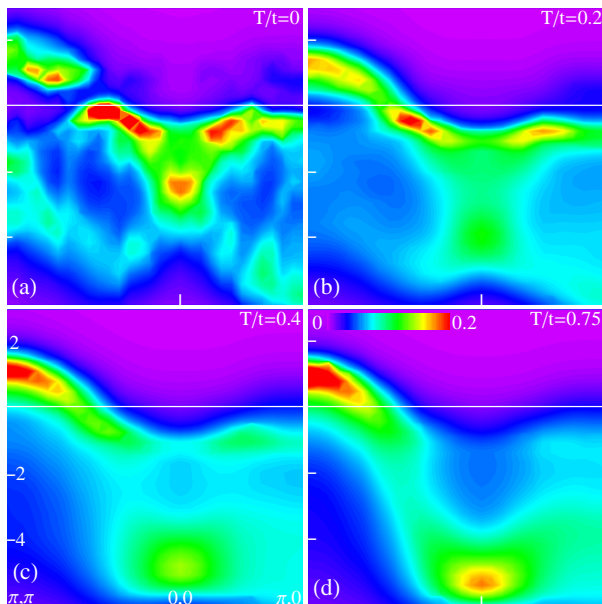


Figure 1: (Color online) Weight map of $A(\mathbf{k}, \omega)$ vs. \mathbf{k} along symmetry lines in the Brillouin zone for $c_h = 0.1$ and different T/t .

If one concentrates on the dispersion along the zone diagonal $(0, 0) - (\pi, \pi)$ it is easy to recognize the HEK feature at $\omega \sim -t$ for all presented T . In fact, a pronounced waterfall-like single band dispersion is evident even at very high $T \sim t > J$, where the steep drop appears close to $\mathbf{k} \sim x(\pi, \pi)$ with $x \sim 0.3$. It should be, however, noted that $T \sim t$ represents already very high T in this doping regime which leads to a substantial shift of the chemical potential so that the Fermi surface is tending towards (π, π) as evident in Fig. 1d.

With lowering $T < J$ the $\omega = 0$ (Fermi surface) crossing of the dispersion along the zone diagonal approaches $\mathbf{k} \sim (\pi/2, \pi/2)$ as expected for low doping. More relevant here, the single dispersion curve evolves into a more complex structure: a) the $\omega > 0$ part not accessible by ARPES reveals a well-defined dispersion of weakly damped QP, b) the renormalized band with small QP velocity remains well defined close to the Fermi surface, i.e. at $\mathbf{k} \sim (\pi/2, \pi/2)$, or even extends nearly to $(0, 0)$ at low $T \rightarrow 0$, c) less coher-

ent band-like feature corresponding roughly to the bottom of the unrenormalized band is well developed close to the zone center, $\mathbf{k} \sim (0, 0)$. For $T < J$ both bands coexist at least at $\mathbf{k} \sim (\pi/4, \pi/4)$.

All observed features are present also in $(\pi, 0) - (0, 0)$ direction as clearly seen in Fig. 1. However, the difference appears at higher T where the entire band in this direction is positioned well below the chemical potential and does not experience the waterfall effect anymore. This is in agreement with the evolution of the band towards the usual although still renormalized tight-binding dispersion.

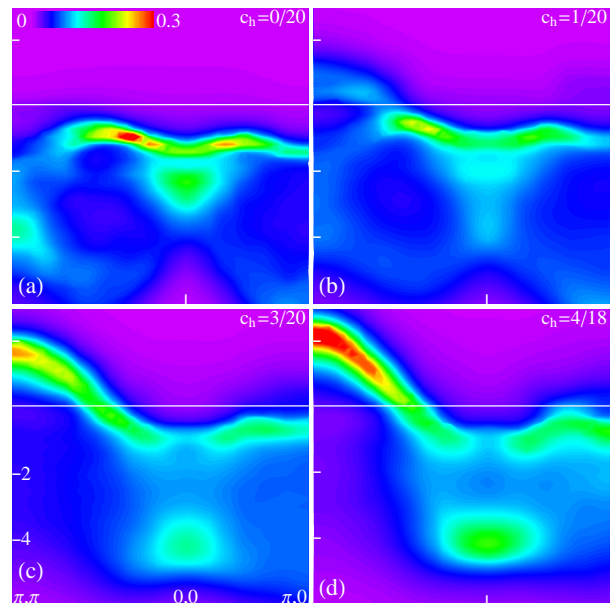


Figure 2: (Color online) Weight map of $A(\mathbf{k}, \omega)$ vs. \mathbf{k} along symmetry lines for fixed $T/t = 0.2$ and different hole dopings c_h .

Quite analogous behavior can be followed at fixed low T as a function of doping. We show results obtained using FTLM for systems with $N = 18, 20$ within a broad doping range $c_h = 0/20 - 4/18$. Note that for the undoped system, $c_h = 0$, the absolute position of the chemical potential is not well defined within the t - J model. In the latter case in Fig. 2a, one can again recognize very well pronounced renormalized QP band reaching the zone center, while the bottom band is very incoherent. Both bands coexist in $(\pi/4, \pi/4) - (0, 0)$ and $(\pi/4, 0) - (0, 0)$ regions. With increasing c_h the renormalized QP band remains well defined near the Fermi surface at $\mathbf{k} \sim (\pi/2, \pi/2)$, but dissolves towards the zone center. At the same time the bottom band starts to move away from the renormalized band and stays well pronounced near $\mathbf{k} \sim (0, 0)$. Both bands are connected with the waterfall-like drop of low intensity. While the whole effective bandwidth is weakly reduced $\Delta\omega \sim 6t < 8t$ relative to a tight-binding band, the bottom of the band at $\mathbf{k} = (0, 0)$ is deeper than expected from the tight-binding dispersion in the case of $c_h = 3/20, 4/18$. This is consistent with experimental observations [3].

The origin of the HEK can be best analyzed and understood by expressing the single-particle Green's function corresponding to $A(\mathbf{k}, \omega) = -\text{Im}G(\mathbf{k}, \omega)$ in terms of the self energy $\Sigma(\mathbf{k}, \omega)$,

$$G(\mathbf{k}, \omega) = \frac{\alpha}{\omega - \zeta_{\mathbf{k}} - \Sigma(\mathbf{k}, \omega)}. \quad (2)$$

The model, Eq.(1), defined with projected fermionic operators requires a nonstandard normalization α as well as a nontrivial 'free' term $\zeta_{\mathbf{k}}$ representing the first frequency moment of the $A(\mathbf{k}, \omega)$ [22]. Within the paramagnetic metal with $\langle \mathbf{S}_i \rangle = 0$ one can express explicitly $\alpha = (1 + c_h)/2$ and

$$\zeta_{\mathbf{k}} = \bar{\zeta} - 4 \sum_j r_j t_j \gamma_j(\mathbf{k}), \quad r_j = \alpha + \frac{1}{\alpha} \langle \mathbf{S}_0 \cdot \mathbf{S}_j \rangle, \quad (3)$$

where $t_j, j = 1, 3$ represent hopping parameters t, t', t'' , respectively, which are renormalized with r_j that involve local spin correlations $\langle \mathbf{S}_0 \cdot \mathbf{S}_j \rangle$. The tight-binding band dispersions corresponding to t_i are then $\gamma_1(\mathbf{k}) = (\cos k_x + \cos k_y)/2$, $\gamma_2(\mathbf{k}) = \cos k_x \cos k_y$ and $\gamma_3(\mathbf{k}) = (\cos 2k_x + \cos 2k_y)/2$. The above expression, Eq.(2), in terms of α and $\zeta_{\mathbf{k}}$ leads to properly analytically behaved $\Sigma(\mathbf{k}, \omega \rightarrow \pm\infty) \propto 1/\omega$.

Following Eq.(2) we extract $\Sigma''(\mathbf{k}, \omega)$ provided that $A(\mathbf{k}, \omega)$ are smooth enough which is for available systems typically the case for $T/t > 0.1$. In Fig. 3 we present results for $\Sigma''(\mathbf{k}, \omega)$ corresponding to spectra in Figs. 1 at $c_h = 2/20$ and various T/t , but fixed $\mathbf{k} = (\pi/4, \pi/4)$ chosen to represent the location of the HEK. It should be noted that $\Sigma''(\mathbf{k}, \omega)$ is not crucially dependent on \mathbf{k} (ignoring here more delicate phenomena as the pseudogap [21]), at least not inside the Fermi volume so results in Fig. 3 are representative for all \mathbf{k} relevant for effective ARPES bands.

Several characteristic properties of the QP damping recognized already in previous studies [20, 21, 22] can be deduced from Fig. 3. a) The damping function $\Sigma''(\mathbf{k}, \omega)$ is very asymmetric with respect to the Fermi energy $\omega = 0$. For the hole-doped case discussed here the damping is large only for $\omega < 0$ corresponding to ARPES. b) As one expects in a metal we find $\Sigma''(\mathbf{k}, \omega = 0) \rightarrow 0$ (or at least decreasing) at low $T \rightarrow 0$, a prerequisite for a well defined Fermi surface. c) Within quite a large regime $-2t < \omega < 0$ we recover at low T well known marginal variation $-\Sigma''(\mathbf{k}, \omega) \propto |\omega|$ [20, 23], while only at large $\omega < -3t$ the damping decreases and loses intensity. e) Increasing T mainly influences the behavior close to $\omega \sim 0$ filling the dip and increasing $|\Sigma''(\mathbf{k}, \omega \sim 0)|$, at the same time making $\Sigma''(\mathbf{k}, \omega)$ more featureless.

Clearly, the strength and the form of $\Sigma''(\mathbf{k}, \omega)$ determines the anomalous dispersion $\omega_{\mathbf{k}}$ via the pole location

$$\omega_{\mathbf{k}} - \zeta_{\mathbf{k}} + \frac{1}{\pi} \int d\omega' \frac{\Sigma''(\mathbf{k}, \omega')}{\omega_{\mathbf{k}} - \omega'} = 0. \quad (4)$$

The relevant quantity to estimate the influence of $\Sigma''(\mathbf{k}, \omega)$ on the dispersion $\omega_{\mathbf{k}}$ is the intensity $\eta_{\mathbf{k}}^2 = -\int \Sigma''(\mathbf{k}, \omega) d\omega/\pi$. We notice that at low doping $\eta_{\mathbf{k}}$ is not strongly dependent either on \mathbf{k} , c_h nor on T . In the range of interest corresponding

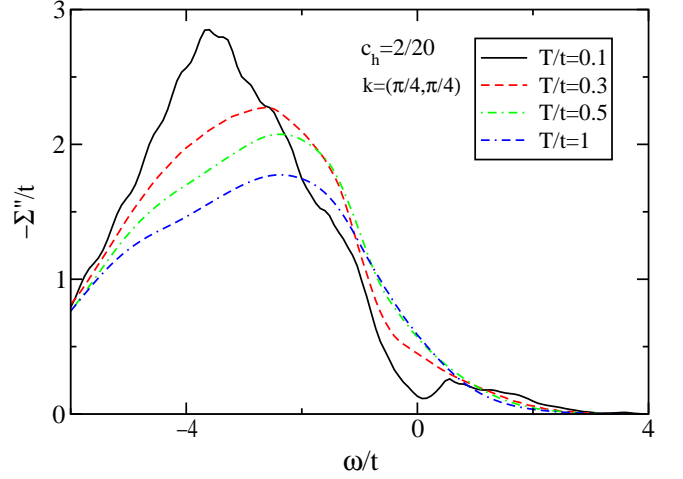


Figure 3: (Color online) Damping function $-\Sigma''(\mathbf{k}, \omega)$ corresponding to Fig. 1 for $c_h = 0.1$, $\mathbf{k} = (\pi/4, \pi/4)$ and various $T/t = 0.1 - 1$.

to Figs. 1-3 we find $\eta_{\mathbf{k}}^2 \sim 3 - 4 t^2$. It should be noted that the origin of large $\eta_{\mathbf{k}}$ is here entirely in strong correlations, i.e., in the incoherent motion of a particle (hole) in a spin background with singly occupied sites. Such physics can be well captured by, e.g., a retracable path approximation [24] where one gets $\eta^2 = 4t^2$, very close to our numerical results.

Since $\zeta_{\mathbf{k}}$ in Eq.(3) produces only a regular although renormalized tight-binding dispersion, the anomalous effective dispersion emerges from $\Sigma'(\mathbf{k}, \omega)$. Due to large $\eta_{\mathbf{k}}$ and a restricted range $-6t < \omega < 0$ of appreciable $|\Sigma''(\mathbf{k}, \omega)|$, $\Sigma'(\mathbf{k}, \omega)$ leads to a substantial change of the dispersion in this ω regime. At low doping and $T < J$ it induces in combination with a narrow $\zeta_{\mathbf{k}}$ a coexistence of renormalized QP band and the bottom band at $\mathbf{k} < (\pi/4, \pi/4)$. The latter one is quite incoherent due to large $|\Sigma''(\mathbf{k}, \omega)|$ in $\omega < 0$ region. On the other hand at $\omega \sim 0$ one has $\Sigma''(\mathbf{k}, \omega) \rightarrow 0$ which allows for a well defined renormalized QP band near the Fermi surface.

The effect of $T > 0$ is to broaden $\Sigma''(\mathbf{k}, \omega)$ and to increase QP damping at $\omega \rightarrow 0$. Then, $\Sigma'(\mathbf{k}, \omega)$ shows less structure and the renormalized QP peak at low ω transforms with increasing T into a single effective band. However, due to T -independent $\eta_{\mathbf{k}}$ the structure of $\Sigma'(\mathbf{k}, \omega)$ remains strong enough to keep the waterfall drop up to very high T . Note that even for larger T as in Figs. 1c,d an effective dispersion following Eq.(3) remains renormalized by $r_j \sim \alpha$ although the band becomes wider as spin correlations loose intensity for $T > J$. Analogous are phenomena at larger doping except that $\Sigma''(\mathbf{k}, \omega)$ generally decreases with c_h .

To illustrate that above features are essential and sufficient to reproduce the HEK and the waterfall we compare numerical results in Fig. 1 with a simplified model of $|\Sigma''(\mathbf{k}, \omega)|$ assuming: a) $\Sigma''(\omega)$ is local, i.e., \mathbf{k} independent, b) at $T = 0$ it follows marginal behavior (linear in ω) for $-\epsilon_a < \omega < 0$ [23], c) for larger binding energies $-\epsilon_b < \omega < -\epsilon_a$ it decreases linearly to zero, d) the effect of $T > 0$ is to convolute $\Sigma''(\omega, T =$

0) with usual thermodynamic factor $f(\omega)[1 - f(\omega)]$ where $f(\omega)$ is the Fermi-Dirac distribution.

For results presented in Fig. 4 we fix $\epsilon_a = t$, $\epsilon_b = 6t$, $\eta = 2t$ and vary $\zeta_{\mathbf{k}}$ through $r_1 = 0.35, 0.5$ for $T = 0, 0.75$, respectively, while $r_{2,3} = \alpha$. We present in Fig. 4 the T -dependence of $A(\mathbf{k}, \omega < 0)$ with \mathbf{k} along the zone diagonal. It is well visible how the two-band structure at low T transforms into a rather regular but broad single band with persistent waterfall even at very high $T \sim t$.

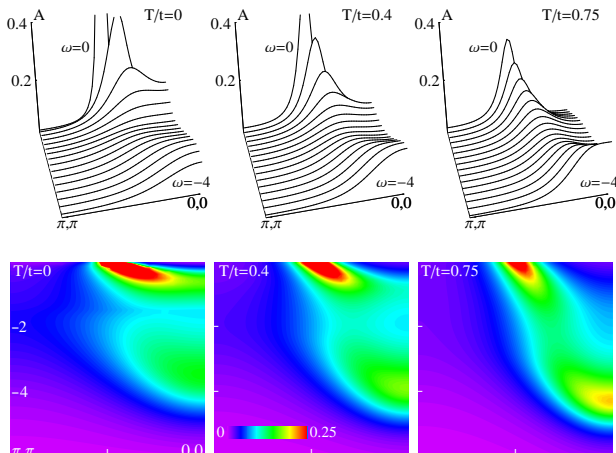


Figure 4: $A(\mathbf{k}, \omega)$ along the zone diagonal calculated from a simplified model and various $T/t = 0, 0.4$ and 0.75 .

In conclusion, we have shown that the prototype model as the extended t - J model incorporates the physics of the HEK as well as the waterfall as observed in numerous recent ARPES studies of hole-doped cuprates. While at low c_h and low T the spectra typically reveal a coexistence of a narrower renormalized QP band and an incoherent bottom band most pronounced at $\mathbf{k} \sim (0, 0)$ the structure evolves with increasing either c_h or T into a single waterfall-like band which persists up to very high $T \sim t$ or in the overdoped regime.

The origin of the anomalous dispersion is according to our analysis entirely due to presence of strong correlations, as incorporated already in the incoherent hole motion in a correlated insulator, as given within the Brinkman-Rice scenario [24]. Such a conclusion offers also the explanation why the waterfall phenomenon persists up to high $T > J$ and in a very broad range of hole doping c_h . Our results also indicate that explanations in terms of specific low- T features as the AFM long range order [12] or AFM fluctuations [16, 17], quantum critical point [14] might be too narrow. In addition, similar waterfall behavior can be observed also in 1D t - J model at high $T > J$ [25]. However, instead of an incoherent bottom band a coherent holon branch emerges with reducing $T < J$.

This is different from the present case in 2D.

There are also some predictions relevant for ARPES experiments emerging from our analysis. In particular, ARPES spectra of electron-doped cuprates should correspond to $\omega > 0$ spectra of hole-doped cuprates (although with opposite t' and t'') as already commented in [26]. From the large asymmetry in ω as seen in presented results it follows that one cannot expect the HEK and waterfall in ARPES results of electron-doped cuprates. Further, our results predict an evolution of the anomalous dispersion with increasing T and c_h , nevertheless the waterfall features should persist up to very high $T > J$ as well as in the overdoped regime.

This work was supported by the Slovenian Research Agency under grant PI-0044. T.T. acknowledges supports from the Next Generation Supercomputing Project of Nanoscience Program, CREST, and Grant-in-Aid for Scientific Research from MEXT, Japan.

-
- [1] A. Damascelli, Z. Hussain, and Z.-X. Shen, *Rev. Mod. Phys.* **75**, 473 (2003).
 - [2] F. Ronning *et al.*, *Phys. Rev. B* **71**, 094518 (2005).
 - [3] W. Meevasana *et al.*, *Phys. Rev. B* **75**, 174506 (2007).
 - [4] J. Graf *et al.*, *Phys. Rev. Lett.* **98**, 067004 (2007).
 - [5] T. Valla *et al.*, *cond-mat/0610249*.
 - [6] J. Chang *et al.*, *cond-mat/0610880*.
 - [7] Z.H. Pan *et al.*, *cond-mat/0610442*.
 - [8] D. S. Inosov *et al.*, *cond-mat/0703223*.
 - [9] B. P. Xie *et al.*, *Phys. Rev. Lett.* **98**, 147001 (2007).
 - [10] S. R. Park *et al.*, *Phys. Rev. B* **75**, 060501(R) (2007).
 - [11] B. J. Kim *et al.*, *Nature Phys.* **2**, 387 (2006).
 - [12] E. Manousakis, *Phys. Lett. A* **362**, 86 (2007).
 - [13] Q.-H. Wang, F. Tan, and Y. Wan, *cond-mat/0610491*.
 - [14] L. Zhu, V. Aji, A. Shekhter, and C. M. Varma, *cond-mat/0702187*.
 - [15] K. Byczuk, M. Kollar, K. Held, Y.F. Yang, I. A. Nekrasov, Th. Pruschke, and D. Vollhardt, *Nature Phys.* **3**, 168 (2007).
 - [16] A. Macridin, M. Jarrell, Th. Maier, and D. J. Scalapino, *cond-mat/0701429*.
 - [17] R. S. Markiewicz *et al.*, *cond-mat/0701524*.
 - [18] T. Tohyama and S. Maekawa, *Phys. Rev. B* **64**, 212505 (2001).
 - [19] T. Tohyama, *Phys. Rev. B* **70**, 174517 (2004).
 - [20] for a review see J. Jaklič and P. Prelovšek, *Adv. Phys.* **49**, 1 (2000).
 - [21] M. M. Zemljič and P. Prelovšek, *Phys. Rev. B* **75**, 104514 (2007).
 - [22] P. Prelovšek and A. Ramšak, *Phys. Rev. B* **63**, 180506(R) (2001); *Phys. Rev. B* **65**, 174529 (2002).
 - [23] C.M. Varma, P.B. Littlewood, S. Schmitt-Rink, E. Abrahams, and A.E. Ruckenstein, *Phys. Rev. Lett.* **63**, 1996 (1989).
 - [24] R. Brinkman and T. M. Rice, *Phys. Rev. B* **2**, 1324 (1970).
 - [25] M. M. Zemljič, P. Prelovšek, and T. Tohyama, unpublished.
 - [26] M. M. Zemljič, P. Prelovšek, and T. Tohyama, *cond-mat/0702644*.